Aerosol and Air Quality Research, 14: 99–107, 2014

ISSN: 1680-8584 print / 2071-1409 online
doi: 10.4209/aaqr.2013.05.0154

Aerosol Characteristics and Radiative Forcing during Pre-Monsoon and Post-Monsoon Seasons in an Urban Environment

Khan Alam[1,2*], Najm us Sahar[1], Yaseen Iqbal[1]

[1] *Institute of Physics and Electronics, University of Peshawar, Khyber Pakhtunkhwa, Pakistan*
[2] *Higher Education Commission (HEC) of Pakistan, Pakistan*

ABSTRACT

The present study reports on aerosol characteristics and radiative properties utilizing ground based Aerosol Robotic Network (AERONET) data for the pre-monsoon (March, April, May) and post-monsoon (September, October, November) seasons over Lahore, Pakistan, for the two years during 2009–2010. The Aerosol Optical Depth (AOD) data from AERONET and a Moderate Resolution Imaging Spectro-radiometer (MODIS) were compared in order to validate both systems. The correlation coefficient for the post-monsoon season was > 0.68 in comparison to > 0.66 for the pre-monsoon season. In the pre-monsoon season, AERONET and MODIS AOD values were in the range of 0.2 to 1.2, and 0.2 to 1.67, respectively. For the post-monsoon season, these values were in the range of 0.17 to 2.46, and 0.15 to 2.45 for AERONET and MODIS, respectively. Strong dust loading resulted in higher values for the coarse particles during the pre-monsoon period, followed by an increase in the absorbing anthropogenic aerosols with the change from the pre-monsoon to post-monsoon season. The higher dust loading corresponded to the higher values of the real part of the refractive index in the pre-monsoon season, causing a relatively large single scattering albedo (SSA) (0.85–0.915) and thus a higher value for the asymmetry parameter (ASY). Similarly, the higher value of absorbing anthropogenic aerosols resulted in a higher value for the imaginary part of the refractive index in the post-monsoon period, followed by relatively lower values for SSA (0.88–0.911) and ASY. The averaged aerosol radiative forcing (ARF) for the pre-monsoon period at the top of the atmosphere was –19 ± 6 W/m^2, while at the surface it was –93 ± 22 W/m^2 leading to an atmospheric forcing of +74 ± 16 W/m^2. Likewise, the averaged ARF for the post-monsoon period at the top of the atmosphere was –28 ± 8 W/m^2, while at the surface it was –98 ± 24 W/m^2 leading to an atmospheric forcing of +70 ± 15 W/m^2, indicating significant heating of the atmosphere.

Keywords: AERONET; MODIS; Pre-monsoon; Post-monsoon; AOD; ARF; SSA; ASY.

INTRODUCTION

In order to have a better understanding of aerosol dynamics and its influence on the global and regional climatic conditions, an adequate knowledge of its spatial and temporal distributions as well as of its variations is very important (Kaufmann *et al.*, 2002; More *et al.*, 2013). For this purpose different ground and satellite based sensing techniques are providing a systematic retrieval of aerosol optical properties on the global and regional scale (Kaufmann *et al.*, 2005; Kahn *et al.*, 2010; More *et al.*, 2013). Aerosol Robotic Network (AERONET), a ground based sensor, provides a columnar aerosol optical depth over the land and ocean; however, its measurement is limited to a smaller area (i.e., point observations) as compared to the Moderate Resolution Imaging Spectro-radiometer (MODIS) Terra (launched 1999) and Aqua (launched 2002), which provides information over a relatively larger spatial domain twice a day (Kaufmann *et al.*, 2002; More *et al.*, 2013). However, chances of error increase in the later, because of the high surface reflectance in certain areas (More *et al.*, 2013). Although the ground based aerosol remote sensing does not provide the global coverage, its wide angular and spectral measurements of solar and sky radiation are best suited for reliable and continuous derived data of aerosol optical properties for key locations (Dubovik *et al.*, 2002). Therefore, in order to improve the accuracy of the MODIS data, it is important to compare and validate the MODIS data with the independent ground based measurements (More *et al.*, 2013).

Several studies have compared and thus evaluated MODIS aerosol products with the ground based aerosol optical depth (AOD) measurements retrieved from AERONET for different areas. Alam *et al.* (2011c) compared the datasets of MODIS and MISR with AERONET for summer and winter seasons of Lahore and Karachi, and found a relatively better correlation between MODIS and AERONET for

* Corresponding author.
Tel.: +92-300-2514177
E-mail address: khanalam@upesh.edu.pk

Lahore (vegetated area), while the correlation for Karachi was found good, in case of MISR and AERONET (coastal area). Similarly several studies on the validation of MODIS derived AODs have also been carried out in India. Tripathi *et al.* (2005) compared MODIS and AERONET AOD and reported that MODIS-derived AODs were over-estimated during dust loading season (September to December) and under-estimated for non-dusty season (January to March), consistent with Prasad and Singh (2007). More *et al.* (2013) compared AOD data for MODIS, MICROTOPS, and AERONET in urban city Pune (India) and found good correlation between MODIS and ground-based measurements with correlation coefficients in the range of 0.62 to 0.93.

Despite similar climatic and geographical conditions at certain areas of Indo-Pak subcontinent like Karachi-Mumbai, Lahore- Delhi, a large number of studies have been carried out to understand the optical and physical properties of aerosols over India; however, only a few studies (Alam *et al.*, 2011a, 2012) could be traced regarding Pakistan. Alam *et al.* (2011a, 2012) reported their findings regarding aerosol optical and radiative behavior over Karachi and Lahore, indicating variations in the aerosol types over Pakistan.

Pakistan is a developing country and lies in the extreme north-west of Indian sub-continent. It has four distinct seasons; winter (December–February), pre-monsoon (March–May), Monsoon (June–August) and post-monsoon (September–November). In the present study, pre- and post-monsoon seasons have been selected because of a significant change in the precipitation and temperature of the region during these periods of the year. This indicates the spatio-temporal variation in aerosol characteristics, generally attributed to the naturally occurring dust particles and contribution of anthropogenic activities. This study carries out an inter-comparison of MODIS aerosol products with AERONET data to understand deviation, if any, in the two data sets at Lahore. AERONET data has also been used to analyze AOD at 550 nm, particle size distribution, single scattering albedo (SSA), asymmetric parameter (ASY) together with the real and imaginary parts of refractive index (RI). The aerosol radiative forcing (ARF) was calculated using Santa Barbra DISORT Atmospheric Radiative Transfer (SBDART) model (Ricchiazzi *et al.*, 1998).

AERONET SAMPLING SITE AND INSTRUMENTATION

Site Description

Lahore (Lat. 31°32′N; Long. 74°22′E) is located close to the Indian boarder, along river Ravi. It is the second mega city of Pakistan with a population of more than 10 million and covers a total land area of 404 sq. Km. The weather of Lahore is largely subjected to four seasons: winter (December to February), Pre monsoon (March to May), monsoon season (June to August), and a post-monsoon period (September to November). May, June, and July are the hottest months, while December, January and February are the coldest months. The mean maximum temperatures in April to June ranges between 33°C and 39°C and in winter these varry from 17 to 22°C. Similarly, the mean minimum temperatures in April to June range between 22 and 28°C while in winter these temperatures vary from 7 to 12°C. Lahore, which is an industrial city, contains major industries manufacturing engineering products, pharmaceuticals, steel, chemicals, construction materials, motor cars and motorcycles. The number of registered vehicles in Lahore is 2.2 million; therefore, vehicular traffic is one of the main sources of atmospheric aerosol. Other anthropogenic sources of aerosols over this sampling site are derived mainly from main highways, coal combustion and biomass burning (Alam *et al.*, 2012). Soil, road dust, and industrial emissions are considered as secondary aerosols (Alam *et al.*, 2011b).

Instrumentation

AERONET

The AERONET, a ground-based remote-sensing aerosol network established by NASA, consists of more than 400 permanent and temporary sites worldwide. One of these sites is Lahore, Pakistan. Lahore AERONET is operational since December 2006 under the joint collaboration between NASA and Pakistan Space and Upper Atmosphere Research Commission (*SUPARCO*), located at Space and Atmospheric Sciences Division, Institute of Space Technology, Lahore.

A CIMEL sun/sky radiometer is the standard AERONET instrument which takes measurements of the direct Sun and diffuse sky radiances within the range from 340 nm to 1020 nm and 440–1020 nm spectral ranges, respectively (Holben *et al.*, 1998). AERONET data are available at three levels; level 1.0 (unscreened), level 1.5 (cloud screened) (Smirnov *et al.*, 2000) and level 2.0 (cloud screened and quality assured) (Holben *et al.*, 1998) and can be downloaded from the AERONET website (http://aeronet.gsfc.nasa.gov/). In the present study we used AERONET level 2.0 (cloud screened and quality assured) data, from both direct sun (AOD and <alpha>) and inversion products (SSA, ASY, RI), during 2009–2010 for the pre-monsoon and post-monsoon seasons. The inversion algorithm is used to retrieve aerosol volume size distributions in the size range $0.05 \le r \le 15$ mm, together with the spectrally dependent complex RI, SSA and ASY parameters from spectral sun and sky radiance data. The detailed aerosol properties retrieved are used for calculating broad brand flux within the spectral range from 0.2 to 4.0 mm (wavelength).

MODIS

The MODIS sensor onboard NASA’s Terra and Aqua satellites were launched in December 1999 and May 2002, respectively. MODIS views in 36 channels from 0.14 µm to 14 µm at different resolutions (250 m, 500 m, and 1000 m). Among the hundreds of products derived from MODIS, measured radiances is suitable for aerosol products (Levy *et al.*, 2007) and cloud products (King *et al.*, 2003; Platnick *et al.*, 2003) including aerosol optical depth (AOD), cloud top pressure and cloud fraction. Aerosol retrieval over land is different from that of the oceans (Tanre *et al.*, 1997); therefore, MODIS aerosol retrievals over land are not expected to be as accurate as over the oceans. The percentage error of measurement from MODIS data is smaller for oceans than that of the land (Remer *et al.*, 2005). MODIS measures AOD with an estimated error of ± 0.05 ± 0.15 (AOD) over the land (Chu *et al.* 2002) and 0.03 ± 0.05 (AOD) over the ocean (Remer *et al.* 2005). High albedo areas such as the Sahara Desert and snow or ice covered regions cause problems for the MODIS instrument leading to a large inclination in models and ground-based observations (Alam *et al.*, 2010). Therefore, the land surface and atmospheric aerosol content are not easy to differentiate due to the fact that both have high reflectance (Wong *et al.*, 2010). In order to improve the accuracy and the quality of retrieved data, the MODIS algorithms have been updated by modifying cloud-masking processes, aerosol models, and the surface reflectance database (Remer *et al.*, 2005; Levy *et al.*, 2007). Deep-Blue algorithm is an important addition to the MODIS Level 2 aerosol product, which is viable to retrieve aerosol properties over bright land surfaces including Sahara Desert. The MODIS provides observations at moderate spatial (250–1 km) and temporal (1–2 days) resolutions over different portions of the electromagnetic spectrum. Several aerosol parameters are also retrieved at a 10 km spatial resolution from MODIS daytime data. More detailed information on algorithms for the retrieval of aerosol and cloud parameters is available at http://modis-atmos.gsfc.nasa.gov. In this study, the monthly mean AOD MODIS Terra Level 2 product with 10 × 10 km spatial resolution was used for two years during 2009–2010.

RESULTS AND DISCUSSION

In the following sub-sections aerosol optical properties, for example AOD, size distribution, RI, SSA, and ASY are discussed in detail. Inter-comparison has been carried out to validate MODIS derived AOD with that of AERONET AOD. In the last section ARF is calculated at the top of the atmosphere, at the earth's surface, and within the atmosphere using radiative transfer model.

Aerosol Optical Depth (AOD)

Aerosol Optical Depth (AOD) which is the degree, to which aerosols prevent the transmission of light through scattering and absorption, can be defined as the integrated extinction co-efficient over a vertical column of unit cross-section. An analysis of the $MODIS_{AOD}$ and $AERONET_{AOD}$ for the pre-monsoon and post-monsoon seasons over Lahore showed that the $MODIS_{AOD}$ and $AERONET_{AOD}$ values ranged from 0.2 to 1.67 and 0.2 to 1.2 during the pre-monsoon period, and from 0.15 to 2.45 and from 0.17 to 2.46 during the post-monsoon period (Fig. 1(a) and (b)). Both AERONET and MODIS AOD are based on the same sampling days during pre-monsoon and post-monsoon seasons. Calculations of the columnar averaged value and the standard deviation of AOD at 550nm have also been carried out for the two data sets. These results showed that the average AOD values for MODIS and AERONET were 0.69 ± 0.25 and 0.54 ± 0.19 for the pre-monsoon and 0.75 ± 0.48 and 0.71 ± 0.46 for the post-monsoon season. These results indicated that the AOD values were comparatively low for both the data sets during the pre-monsoon season in comparison to the post-monsoon season. In general, the AOD values for MODIS were found to be relatively compatible with that of AERONET during the pre-monsoon, but in the month of May these values showed a relatively

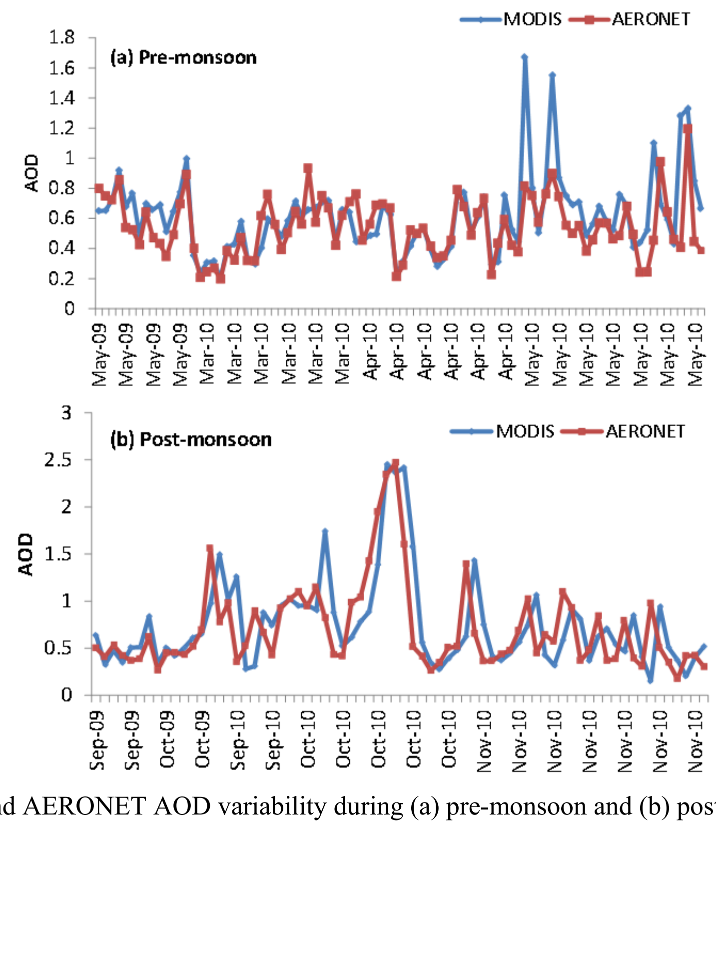

Fig. 1. MODIS and AERONET AOD variability during (a) pre-monsoon and (b) post-monsoon seasons.

higher over-estimation for MODIS (Fig. 1(a)). On the other hand, although, the AOD values were higher for the two data sets during the post-monsoons, yet these values were rather compatible. Alam *et al.* (2011c) analyzed AOD at 550 nm for different cities of Pakistan during 2002–2008 and reported higher AOD values for summer followed by spring, autumn and winter seasons. Similarly, Ranjan *et al.* (2007) reported higher AOD values for summer than winter. The observation of relatively lower values for winter was attributed to the washout processes due to heavy rains, while the relatively higher AOD values for were related to the heavy winds that drive dust particles. Gupta *et al.* (2003) also reported higher AOD values during pre-monsoon season than winter over Indore (India). Seasonally varying relative abundance of light scattering and absorbing composition and relative humidity can also affect the seasonal variability in AOD values. The high temperature during summer was reported to play a vital role in heating and lifting loose material from soil due to high wind speeds; consequently, higher AOD values were observed during summer (Alam *et al.*, 2011a).

Inter-Comparison of $MODIS_{AOD}$ and $AERONET_{AOD}$

An inter-comparison of AOD values from different satellite sensors is very important to a) establish long-term database for climatological studies, and b) improve the accuracy and coverage achievable with a single sensor (Prasad and Singh, 2007; Alam *et al.*, 2011c). The daily $MODIS_{AOD}$ and daily average of all available $AERONET_{AOD}$ data values are used for both the pre-monsoon and post-monsoon seasons over Lahore. For this purpose, the daily mean AODs of 500 nm from AERONET were first interpolated to a common wavelength of 550 nm of MODIS, using the power law

$$AOD_{550nm} = AOD_{500nm}\,(550/500)^{-\alpha} \quad (1)$$

where α is Ångström exponent at wavelength (440–870 nm) (Prasad *et al.*, 2007; Alam *et al.*, 2011c). Alpha is determined from the spectral dependence of the measured optical depth as suggested by Ångström (1963). Fig. 2(a) and (b) shows the comparison of MODIS and AERONET AOD for pre-monsoon and post-monsoon seasons during the period 2009–2010. The correlation coefficients measured were 0.66 and 0.68 for the pre-monsoon and post-monsoon seasons, respectively. Thus the correlation was almost the same, showing a relatively higher correlation for the post-monsoon season than that of the pre-monsoon period.

A comparison of the linear regression parameters (slope and intercept) of the collocated data (Fig. 2(a) and (b)) is of vital importance (Misra *et al.*, 2008; Levy *et al.*, 2010; More *et al.*, 2013). The deviation of the slope of the plotted data from unity demonstrated the some inconsistency in the MODIS retrievals (Zhao *et al.*, 2002; Tripathi *et al.*, 2005). The measured values of slopes for the post-monsoon and pre-monsoon seasons were 0.72 and 0.87, with correspondence intercepts of +0.243 and +0.134, respectively. The slope of

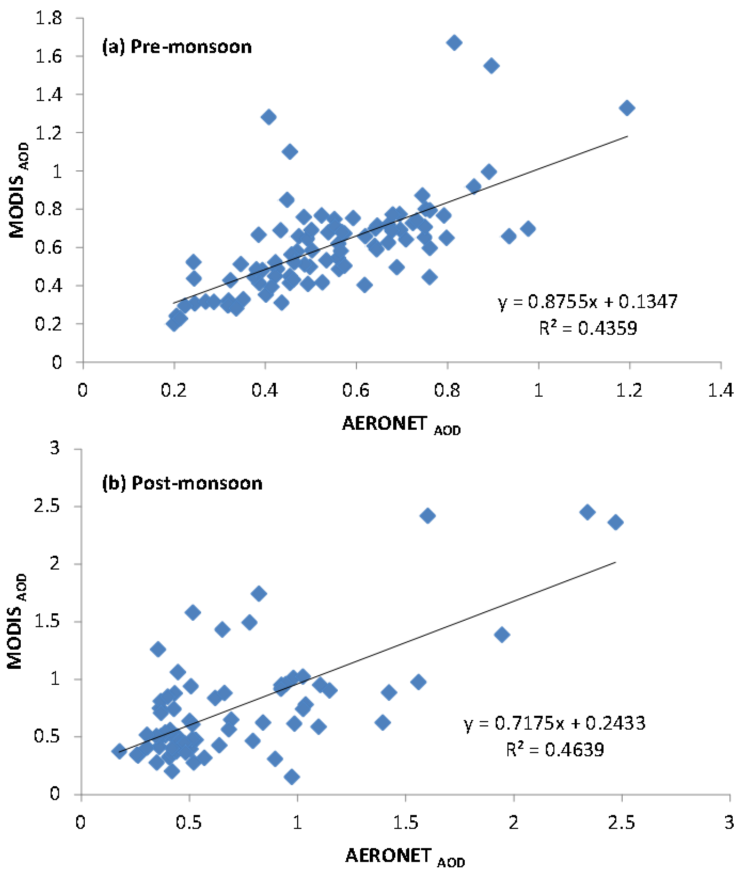

Fig. 2. Inter-comparison of MODIS and AERONET AOD during (a) pre-monsoon and (b) post-monsoon seasons.

pre-monsoon showed that the AOD values for MODIS and AERONET were approximately comparable during the major part of the season, except for a few days when there was an over-estimation of the MODIS AODs. Similarly, the lower value (< 1) of the slope during the post-monsoon season indicated an under-estimation of AOD by MODIS with respect to AERONET retrievals. The non-zero intercepts of these slopes may be attributed to the biasing of the algorithm towards the low AOD values (Zhao *et al.*, 2002; Tripathi *et al.*, 2005; More *et al.*, 2013). The factors contributing to these imperfections may be improper assumptions of surface reflectance and selection of aerosol types. This can also be due to point measurements (AERONET) vs. 10-km grid (MODIS) average retrievals.

Researchers have been working on the inter-comparison among retrievals of a number of data sets. Alam *et al.* (2011c) utilized data from $MISR_{AOD}$ and $MODIS_{AOD}$ and compared these with $AERONET_{AOD}$ for different cities of Pakistan for the period extending from 2002 to 2008. The study showed that MISR performed better for areas close to ocean, while MODIS worked excellently for the vegetated regions. Furthermore, there was good correlation ($R^2 = 0.67$) for $MISR_{AOD}$ and $AERONET_{AOD}$ for Karachi. This study reported a good correlation co-efficient ($R^2 = 0.67$) between MISR and AERONET for Karachi, while, the correlation coefficient was relatively higher ($R^2 = 0.72$) for $MODIS_{AOD}$ and $AERONET_{AOD}$ for Lahore. More *et al.* (2013) found a good match for pre-monsoon (slope ≈ 1 and intercept ≈ 0) for $MODIS_{AOD}$ with $AERONET_{AOD}$; however, for winter the retrievals of the former were under-estimated. In a similar study, Tripathi *et al.* (2005) showed a good correlation during winter and post-monsoon period when there was no-dust loading.

Aerosol Volume Size Distribution (VSD)

The aerosol volume size distribution (VSD) is an important parameter, which has an intense effect on climate. In the present study, AERONET size distribution was determined using 22 bins radius and was reported to range from 0.05 µm to 15 µm. Fig. 3 illustrates pre-monsoon and post-monsoon variation in average volume size distribution for the period during 2009–2010. The VSD has a two-mode structure, which can be characterized by the sum of two lognormal distributions as follows:

$$\frac{dV(r)}{dlnr} = \sum_{i=1}^{2} \frac{C_{v,i}}{\sqrt{2\pi}\sigma_i} \exp\left[-\frac{\left(lnr - lnr_{v,i}\right)^2}{2\sigma_i^2}\right] \quad (2)$$

where σ_i is the standard deviation, $r_{v,i}$ is the volume median radius and $C_{v,i}$ is the volume concentration for fine and coarse modes (Xia *et al.*, 2005; Zheng *et al.*, 2008; Alam *et al.*, 2011a). It is evident from Fig. 3 that the size distribution in the fine mode is dominant at 0.15 µm, whereas the coarse mode is dominant with a 3 µm radius. Alam *et al.* (2011a) found similar results for mega-city Karachi. The VSDs in the course mode were higher in pre-monsoon season than the post-monsoon season; the higher values in pre-monsoon suggested strong dust loading during the

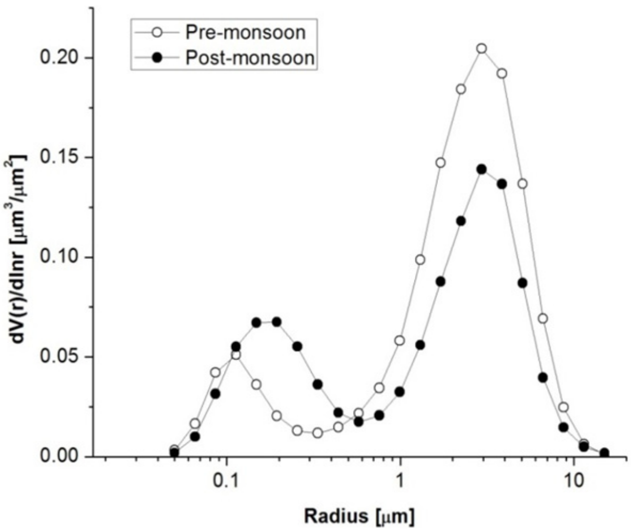

Fig. 3. AERONET aerosol volume size distribution during pre-monsoon and post-monsoon seasons.

season from Thar Desert (India). On the other hand, VSDs in the fine mode were higher in the post-monsoon season than in the pre-monsoon season. The fine mode size distribution indicated that the fine peak radius increased from that of the pre-monsoon (0.11 µm) to the post-monsoon (0.15 µm) season which indicated an anthropogenic aerosol increase from the pre-monsoon to the post-monsoon season. Tripathi *et al.* (2005) reported 50% increase in volume concentration in the coarse mode during the pre-monsoon season in comparison to the other seasons due to dust loading. Wang *et al.* (2011) reported an increasing trend in the fine size mode peak radius from pre-monsoon (0.11 µm) season to the post-monsoon (0.15 µm) and winter seasons (0.19 µm) for Kanpur (India). Pandithurai *et al.* (2008) found that VSD in coarse mode increased from March to May (during pre-monsoon) in New Delhi, India.

Refractive Index

The real and imaginary parts of refractive index (RI) provide information about the scattering and absorbing behavior of aerosols. The higher real part values correspond to the scattering types and the higher imaginary values correspond to the absorbing type aerosol (Sinyuk *et al.*, 2003; Alam *et al.*, 2012). The greatest information about RI comes from aureole radiances, which is strongly affected due to errors in the angle-pointing bias. In the real part of RI, the estimated error is ± 0.04, while 30–50% errors occur in the imaginary part of RI. Fig. 4(a) shows the pre-monsoon and post-monsoon averaged real parts of aerosol refractive index at 440 nm, 675 nm, 870 nm and 1020 nm. The values of the real part of RI were larger at higher wavelengths than those at shorter wavelengths due to higher absorption by coarse particles in the near infrared band (Cheng *et al.*, 2006a, b). The values of the real part of RI in the pre-monsoon were greater than the post-monsoon season, which may be associated with the dust events, complex mineralogy during long range transport and high relative humidity (Alam *et al.*, 2011a). The real part of refractive index of dust aerosol is usually greater than that of the anthropogenic aerosols (Liu *et al.*, 2008; Alam *et al.*, 2011a).

Fig. 4(b) shows the observed variation in the imaginary part of RI with respect to wavelength. The imaginary part values decreased with an increase in wavelength. The average imaginary part values for pre-monsoon season were measured to be between 0.010 ± 0.003 at 440 nm to 0.005 ± 0.002 at 1020 nm, and for the post-monsoon season these values varied from 0.012 ± 0.005 at 440 nm to 0.007 ± 0.003 at 1020 nm. The observed higher imaginary part values at shorter wavelengths may be due to the absorption of organic/black carbon (Arola *et al.*, 2011; Alam *et al.*, 2012). The average values of the imaginary part of RI at all wavelengths were greater for the post-monsoon season than the pre-monsoon season. The higher values may be due to the absorbing anthropogenic aerosols and the lower values indicated the existence of dust aerosols (Alam *et al.*, 2012).

Single Scattering Albedo (SSA) and Asymmetric Parameter (ASY)

Both the SSA and ASY are the key parameters for the assessment of aerosol radiative forcing (Alam *et al.*, 2012).

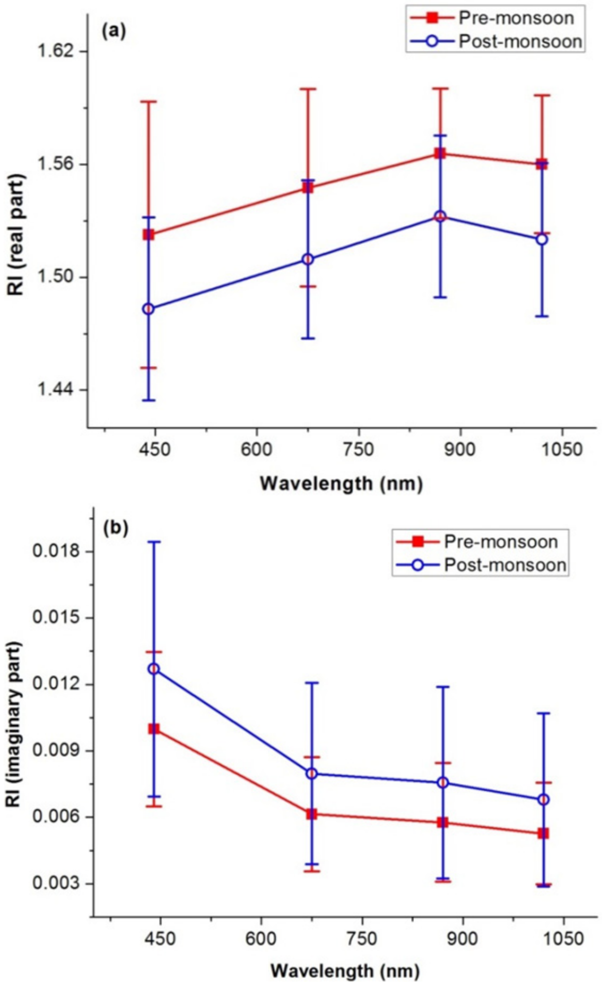

Fig. 4. Spectral variations of the refractive index of (a) real parts and (b) imaginary parts during pre-monsoon and post-monsoon seasons.

contribution of absorption to the extinction. It has thus a vital Being a function of wavelength, SSA is the measure of role in understanding the climatic effects of the aerosols. The values of SSA strongly depend on the aerosol composition and size distribution (Jacobson, 2000; Dubovik *et al.*, 2002; More *et al.*, 2013). Lower values of SSA at longer wavelengths indicate the presence of absorbing aerosols (anthropogenic activities like biomass burning, vehicular emission and industrial pollutants) in abundance, whereas higher values of SSA may indicate the dominance of the coarse (dust) particles which may be attributed to activities like heavy industrialization, rapid urbanization and local activities such as construction (Devara *et al.*, 2002; Devara *et al.*, 2005; Ramchandran and Rajesh, 2007; Bhawar, 2008; Babu *et al.*, 2010; Dani *et al.*, 2010; Kumar *et al.*, 2011; Alam *et al.*, 2012; More *et al.*, 2013).

Fig. 5(a) and (b) shows the spectral variations in averaged SSA and ASY at wavelengths of 440 nm, 675 nm, 870 nm, and 1020 nm during pre- and post-monsoon seasons. The averaged SSA for the pre-monsoon season were measured to be 0.85 ± 0.18 at a wavelength of 440 nm and 0.92 ± 0.02 at a wavelength of 1020 nm, whereas, for the post-monsoon period it was 0.88 ± 0.03 at a wavelength of 440 nm and 0.91 ± 0.02 at a wavelength of 1020 nm. Fig. 5(a) shows that during the pre-monsoon season, SSA increased rapidly with increasing wavelength, which reflected the dominance of scattering particles (dust) over the absorbing particles (anthropogenic pollutants). Similar results were reported (Alam *et al.*, 2012) in his study over Lahore and Karachi for summer (April–June) 2010–2011 season. Fig. 5(a) shows SSA variations for the post-monsoon season. The analysis reveals a gradual increase in the SSA with increasing wavelength, this shows that ratio of absorbing aerosols during this period of year have increased to some extent. Alam *et al.* (2012) and Singh *et al.* (2010) reported a decrease in the SSA with increase in wavelength during winter season.

Likewise SSA, ASY is also a spectral dependent parameter. Fig. 5(b) shows that ASY values decreases with increasing wavelengths. The average ASY during pre-monsoon season was 0.71 ± 0.02 at 440 nm and 0.70 ± 0.02 at 1020 nm, whereas, in post-monsoon the average ASY was 0.72 ± 0.02 at 440 nm and 0.64 ± 0.03 at 1020 nm. The greater decrease in ASY was thus observed for the post-monsoon (September to November). Similar to the results found by Alam *et al.* (2012) for winter season in Lahore and Karachi. The results suggest that during this period of the year the anthropogenic (absorbing) pollutants were relatively in abundance.

Aerosol Radiative Forcing (ARF)

The presence of dust in the atmosphere either scatters or absorbs the ultraviolet (UV), infra-red (IR) and visible radiations depending upon the nature of the dust and on the optical properties of the aerosols. The aerosol radiative forcing (ARF) at the top of the atmosphere (TOA) and at the surface is defined as the net flux (down minus up) measured in W/m^2 with and without aerosol at TOA and at the surface.

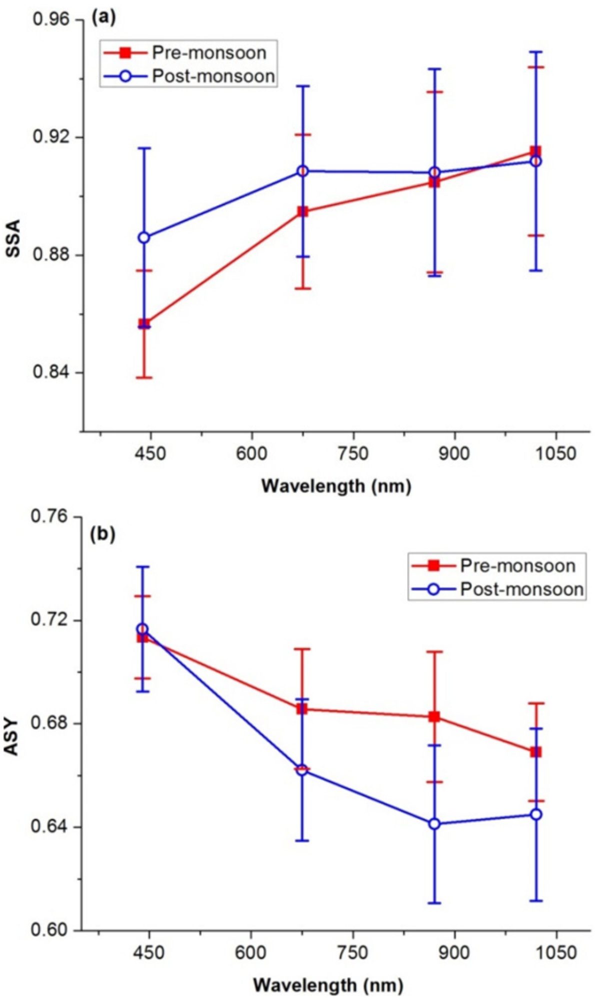

Fig. 5. Spectral variations of (a) Single scattering albedo and (b) Asymmetry parameter during pre-monsoon and post-monsoon seasons.

Scattering of the radiation may result in the cooling effect of the atmosphere (negative forcing) and absorption may lead to the heating of atmosphere (positive forcing). This heating and cooling of the atmosphere due to radiative forcing directly effects the monsoon circulation (Prasad *et al.*, 2007). Since the optical properties play a vital role in determining the radiative forcing of the atmosphere, however, the lack of detailed knowledge of these optical properties may result in an uncertainty in assessing the climatic forcing (Charlson *et al.*, 1992; Houghton *et al.*, 1996; Hansen *et al.*, 1997; Heintzenberg *et al.*, 1997; Hansen *et al.*, 2000; Dubovik *et al.*, 2007). In recent years, however, a number of studies have been conducted that helped us reduce the uncertainties in the direct aerosol radiative forcing (IPCC, 2007). In modeling of aerosol effects on atmospheric radiation, following aerosol optical properties like AOD, SSA, ASY and surface-albedo are important input parameters. The AOD, SSA, ASY values were obtained from Lahore, AERONET site and surface albedo values were obtained from MODIS data over Lahore. One other such parameter is the solar zenith angle, which is calculated by using a small code in the SBDART (Santa Barbra Disort Atmospheric Radiative Transfer) model specifying a particular date, time, latitude and longitude (Alam *et al.*, 2012).

Table 1. Average Aerosol Radiative forcing (ARF) at the TOA, at the earth's Surface and within the Atmosphere.

Seasons	ARF (W/m^2) ± SD		
	TOA	Surface	Atmosphere
pre-monsoon	–19 ± 6	–93 ± 22	+74 ± 16
post-monsoon	–28 ± 8	–98 ± 24	+70 ± 15

The daily averaged TOA and surface forcing have been estimated for the Pre and post-monsoon during 2009–2010. The results showed that surface ARF values ranged from –31 to –145W/m^2 for the pre-monsoon period and from –30 to –160 W/m^2 for the post-monsoon season. The pre-monsoon and post-monsoon season ARF values at TOA were found to be –8 to –35 W/m^2 and –15 to –60 W/m^2 respectively. Likewise the atmospheric ARF values for the pre- and post-monsoon were calculated to be +23 to +105 W/m^2 and +15 to +100W/m^2 respectively. The average ARF at the surface, TOA and within the atmosphere are given in Table 1. The averaged ARF values at the surface during the pre- and post-monsoon periods were –93 ± 22 W/m^2 and –98 ± 24 W/m^2, respectively. Similarly the averaged TOA forcing was –19 ± 6 W/m^2 and 28 ± 8 W/m^2 for the pre- and post-monsoon seasons, respectively. The averaged atmospheric forcing for the pre-monsoon and post-monsoon seasons was +74 ± 16 W/m^2 and +70 ± 15 W/m^2, respectively. Significant differences between surface and TOA forcing indicated that there was a greater absorption of solar radiation within the atmosphere, as a consequence of which the warming of the atmosphere and cooling of surface (Earth) took place (Alam *et al.*, 2012). The values calculated for Lahore in the present study are comparable with those (74.5 ± 16.8 and 41.85 ± 6.4) reported by Alam *et al.* (2012) for Lahore and Karachi during the period 2010–2011. The high positive value indicates significant heating of the atmosphere. Prasad *et al.* (2007) reported ARF values in the range of –29.5 to –87.5 W/m^2 (average –57.5 W/m^2) at the surface and –2.9 to –26 W/m^2 (average –13.5 W/m^2) at TOA for dust loading season, and –19.5 to –52.4 W/m^2 (average –34.5 W/m^2) and +2 to –10 W/m^2 (average –2.5 W/m^2) for non dust loading season, respectively, over Indo-Gangetic plains (India). Hence due to the enhancement of dust aerosols during pre-monsoon season (March to May), the average surface forcing changed by –23 W/m^2 and –11 W/m^2 at the surface and TOA respectively.

CONCLUSION

The aerosol characteristics and their optical properties were analyzed using AERONET and MODIS measurements for the two years period during 2009–2010. The aerosol optical and radiative properties changed from pre-monsoon to post-monsoon season. The $AERONET_{AOD}$ and $MODIS_{AOD}$ showed slightly better correlation for the post-monsoon than the pre-monsoon season. The volume size distribution indicated a higher concentration of coarse mode for the pre-monsoon period, due to high dust loading from the nearby Thar Desert (India). SSA values were higher in pre-monsoon than post-monsoon season due to dust activities in the eastern part of Pakistan. The average atmospheric forcing during the pre-monsoon and post-monsoon was +74 ± 16 W/m^2 and +70 ± 15 W/m^2, respectively. The high atmospheric forcing values indicated maximum absorption of radiation by the atmosphere and hence much heating of the atmosphere. This may be attributed to the mixing of absorbing black-carbon (BC) with that of the moderately absorbing dust.

ACKNOWLEDGEMENTS

The authors acknowledge the financial support of the Higher Education Commission of Pakistan (HEC) for the Project titled "Satellite and ground-based aerosol characteristic in Pakistan: implication to climatic effect". The authors are grateful to the MODIS (http://modis.gsfc.nasa.gov/) teams at NASA for the provision of satellite data, NASA and Institute of Space Technology, Lahore office for providing AERONET data (http://aeronet.gsfc.nasa.gov/).

REFERENCES

Alam, K., Trautmann, T. and Blaschke, T. (2011a). Aerosol Optical Properties and Radiative Forcing over Mega-City Karachi. *Atmos. Res.* 101: 773–782.

Alam, K., Blaschke, T., Madl, P., Mukhtar, A. and Hussain, M., Trautmann, T. and Rahman, S. (2011b). Aerosol Size Distribution and Mass Concentration Measurements in Various Cities of Pakistan. *J. Environ. Monit.* 13: 1944–1952.

Alam, K., Qureshi, S. and Blaschke, T. (2011c). Monitoring Spatio-Temporal Aerosol Patterns over Pakistan Based on MODIS, TOMS and MISR Satellite Data and a HYSPLIT Model. *Atmos. Environ.* 45: 4641–4651.

Alam, K., Trautmann, T., Blaschke, T. and Majid, H. (2012). Aerosol Optical and Radiative Properties during Summer and Winter Season over Lahore and Karachi. *Atmos. Environ.* 50: 234–245.

Ångström, A. (1961). Techniques of Determining the Turbidity of the Atmosphere. *Tellus* 8: 214–223.

Arola, A., Schuster, G., Myhre, G., Kazadzis, S., Dey, S. and Tripathi, S.N. (2011). Inferring Absorbing Organic Carbon Contents from AERONET Data. *Atmos. Chem. Phys.* 11: 215–225.

Bhawar, R.L. (2008). Aerosol Characterization from Satellite and Ground-based Measurements, Ph.D. Thesis, University of Pune, Pune.

Babu, S.S., Sreeranth, V., Nair, V.S., Sateesh, S.K. and Krishnamoorthy, K. (2010). Vertical Profile of Aerosol Single Scattering Albedo over West Coast of India during W_ICARB. *J. Atmos. Sol. Terr. Phys.* 72: 876–882.

Charlson, R.J., Schwartz, S.E., Hales, J.M., Cess, R.D., Coakley, J.A. Jr., Hansen, J.E. and Hofmann, D.J. (1992). Climate forcing by Anthropogenic Aerosol. *Science* 55: 423–430.

Cheng, T., Wang, H., Xu, Y., Li, H. and Tian, L. (2006a). Climatology of Aerosol Optical Properties in Northern China. *Atmos. Environ.* 40: 1495–1509.

Cheng, T., Liu, Y., Lu, D., Xu, Y. and Li, H. (2006b). Aerosol Properties and Radiative Forcing in the Hun Shan Dake Desert, Northern China. *Atmos. Environ.* 40: 2169–2179.

Chu, A., Strabola, K., Planick, S., Moody, E., King, M., Mattoo, S. and Ridgway, B. (2002). MODIS Atmosphere QA Plan, EOS Project. Off., NASA Goddard Space Flight Center.

Dubovik, O., Holben, B. N., King, M.D., Tanre, D. and Slutsker, I. (2002). Variability of Absorption and Optical Properties of Key Aerosol Types Observed in World Wide Locations. *J. Atmos. Sci.* 59: 590–608.

Dani, K.K., Raj, P.E., Devara, P.C.S., Pandithurai, G., Sonbawne, S.M., Maheskumar, R.S., Saha, S.K. and Rao, Y.J. (2012). Long-Term Trends and Variability in Measurement Multi-Spectral Aerosol Optical Depth over a Tropical Urban Station in India. *Int. J. Climatol.* 32: 153–160.

Devara, P.C.S., Maheskumar, R.S., Raj, P.E., Pandithurai, G. and Dani, K.K. (2002). Recent Trends in Aerosol Climatology and Air Pollution as Infrared from Multi-Year Idar Observation over a Tropical Urban Station. *Int. J. Climatol.* 22: 435–449.

Devara, P.C.S., Saha, S.K., Raj, P.E., Sonbawne, S.M., Dani, K.K., Tiwari, Y.K. and Maheskumar, R.S. (2005). A Four-Year Climatology of Total Column Tropical Urban Aerosol, Ozone and Water Vapor Distributions over Pune, India. *Aerosol Air Qual. Res.* 5: 20673–20696.

Gupta P., Gadhavi, H. and Jayaraman, A. (2003). Aerosol Optical Depth Variation Observed Using Sun Photometer over Indore. *Indian J. Radio Space Phys.* 32: 229–237.

Hansen, J., Makiko, S. and Reto. R. (1997). Radiative Forcing and Climate Response. *J. Geophys. Res.* 102: 6831–6864.

Hansen, J., Makiko, S., Reto. R., Andrew, L. and Valder, O. (2000). Global Warming in the Twenty-First Century: An Alternative Scenario. *Proc. Nat. Acad. Sci. U.S.A.* 97: 9875–9880.

Heintzenberg, J., Charlson, R.J., Clarke, A.D., Liousse, C., V. Ramaswamy, V., Shine, K.P., Wendisch, M. and Helas, G. (1997). Measurements and Modeling of Aerosol Single Scattering Albedo: Progress, Problems and Prospects. Beitr. *Phys. Atmos.* 70: 249–263.

Houghton, J.T., Miera Filho, L.G., Callander, B.A., Harris, N., Kattenberg, A. and Maskell, K. (1996). *Climate Change 1995: The Science of Climate Change*, Cambridge University Press, 552 pp.

Holben, B.N., Eck, T.F., Slutsker, I., Tanré, D., Buis, J.P., Setzer, A., Vermote, E., Reagan, J.A., Kaufman, Y.J., Nakajima, T., Lavenu, F., Jankowiak, I. and Smirnov, A. (1998). AERONET-A Federated Instrument Network and Data Archive for Aerosol Characterization. *Remote Sens. Environ.* 66: 1–16.

Holben, B.N., Eck, T.F., Slutsker, I., Tanré, D., Buis, J.P., Setzer, A., Vermote, E., Reagan, J.A. and Jacobson, M.Z. (2000). A Physically Based Treatment of Elemental Carbon Optics: Implications for Global Direct Forcing of Aerosols. *Geophys. Res. Lett.* 27: 217–220.

Kaufman, Y.J., Koren, I., Remer, L.A., Rosenfield, D. and Rudich, Y. (2005). The Effect of Smoke Dust and Pollution Aerosol on Shallow Cloud Development over the Atlantic Ocean. *Proc. Nat. Acad. Sci. U.S.A.* 102: 11207–11212.

Kaufmann, Y.J., Tanre, D. and Boucher, O. (2002). Satellite View of Aerosol in the Climate System. *Nature* 419: 215–223.

King, M.D., Menzel, W.P., Kaufman, Y.J., Tanre, D., Gao, B.C., Platnick, S., Ackerman, S.A., Remer, L.A., Pincus, R. and Hubanks, P.A. (2003). Cloud and Aerosol Properties, Perceptible Water, and Profiles of Temperature and Humidity from MODIS. *IEEE Trans. Geosci. Remote Sens.* 41: 442–458.

Kahn, R.A., Gaitley, B.J., Garay, M.J., Diner, D.J., Eck, T.F., Smirnov, A. and Holben, B.N. (2010). Multiangle Imaging SpectroRadiometer Global Aerosol Product Assessment by Comparison with the Aerosol Robotic Network. *J. Geophys. Res.* 115: D23, doi: 10.1029/2010 JD014601.

Kumar, S., Devara, P.C.S., Dani, K.K., Sonbawne, S.M. and Saha, S.K. (2011). Sun-Sky Radiometer Derived Column-Integrated Aerosol Optical and Physical Properties over a Tropical Urban Station during 2004–2009. *J. Geophys. Res.* 116: D10, doi: 10.1029/2010JD014944.

Levy, R.C., Remer, L.A. and Dubovik, O. (2007). Global Aerosol Optical Properties and Application to Moderate Resolution Imaging Spectroradiometer Aerosol Retrieval over Land. *J. Geophys. Res.* 112, D13210, doi: 10.102 9/2006JD007815, 2007.

Levy, R.C., Remer, L.A., Kleidman, R.G., Mattoo. S., Ichoku, C., Kahn, R. and Eck, T.F. (2010). Global Evaluation of the Collection 5 MODIS Dark-Target Aerosol Products over Land. *Atmos. Chem. Phys.*10: 10399–10420.

Liu, J., Zheng, Y., Li, Z. and Wu, R. (2008). Ground-Based Remote Sensing of Aerosol Optical Properties in One City in Northwest China. *Atmos. Res.* 89: 194–205.

Misra, A., Jayaraman, A. and Ganguly, D. (2008). Validation of MODIS Derived Aerosol Optical Depth over Western India. *J. Geophys. Res.* 113, D04203, doi: 10.1029/2007JD 009075, 2008.

More, S., Kumar, P.P., Gupta, P., Devara, P.C.S. and Aher, G.R. (2013). Comparison of Aerosol Products Retried from AERONET, MICROTOPS and MODIS over a Tropical Urban City, Pune, India. *Aerosol Air Qual. Res.* 13: 107–121.

Platnick, S., King, M.D., Ackerman, S.A., Menzel, W.P., Baum, B.A., Riedi, J.C. and Frey, R.A. (2003). The MODIS Cloud Products: Algorithms and Examples from Terra. *IEEE Trans. Geosci. Remote Sens.* 41: 459–473.

Pandithurai, S., Dipu, S., Dani, K.K., Tiwari, S., Bisht, D.S., Devara, P.C.S. and Pinker, T.R. (2008). Aerosol Radiative Forcing during Dust Events over New Delhi, India. *J. Geophys. Res.* 113. doi: 0.1029/2008JD009804.

Prasad, A.K., Singh, S., Chauhan, S.S., Srivastava, M.K., Singh, R.P. and Singh, S. (2007). Aerosol Radiative Forcing over Indo-Gangetic plains During Major Dust Storms. *Atmos. Environ.* 41: 6289–6301.

Remer, L.A., Kaufman, Y.J., Tanre, D., Matto, S., Chu, D.A., Martins, J.V., Li, R.R., Ichoku, C., Levy, R.C., Kleidman, R.G., Eck, T.F., Vermote, E. and Holben, B.N. (2005). The MODIS Aerosol Algorithm, Products, and Validation. *J. J. Atmos. Sci.* 62: 947–973.

Ricchiazzi, P., Yang, S., Gautier, C. and Sowle, D. (1998). SBDART: A Research and Teaching Software Tool for Plane-Parallel Radiative Transfer in the Earth's Atmosphere. *Bull. Am. Meteorol. Soc.* 79: 2101–2114.

Ranjan, R.R., Joshi, H.P. and Iyer, K.N. (2007). Spectral Variation of Total Column Aerosol Optical Depth over Rajkot: A Tropical Semi-Arid Indian Station. *Aerosol Air Qual. Res.* 7: 33–45.

Sinyuk, A., Torres, O. and Dubovik, O. (2003). Combined Use of Satellite and Surface Observations to Infer the Imaginary Part of the Refractive Index of Saharan Dust. *Geophys. Res. Lett.* 30: 1081, doi: 10.1029/2002GL01 6189.

Smirnov, A., Holben, B.N., Eck, T.F., Dubovik, O. and Slutsker, I. (2000). Cloud Screening and Quality Control Algorithms for the AERONET Data Base. *Remote Sens. Environ.* 73: 337–349.

Tripathi, S.N., Dey, S., Chandel, A., Srivastava, S., Singh, R.P. and Holben, B.N. (2005). Comparison of MODIS and AERONET Derived Aerosol Optical Depth over Ganga Basin, India. *Ann. Geophys.* 23: 1093–1101.

Tanre, D., Kaufman, Y.J., Herman, M. and Mattoo, S. (1997). Remote Sensing of Aerosol Properties over Oceans Using the MODIS/EOS Spectral Radiance. *J. Geophys. Res.* 102: 16971–16986.

Wong, M. S., Lee, K.H., Nichol, J.E. and Li, Z. (2010). Retrieval of Aerosol Optical Thickness Using MODIS 500 X 500 m^2, a Study in Hong Kong and the Pearl River Delta Region. *IEEE Trans. Geosci. Remote Sens.* 48: 3318–3327.

Wang, S., Fang, L., Gu, X., Yu, T. and Geo, J. (2011). Comparison of Aerosol Optical Properties from Beijing and Kanpur. *Atmos. Environ.* 45: 7406–7414.

Xia, X., Wang, P., Chen, H., Philippe, G. and Zhang, W. (2005). Ground Based Remote Sensing of Aerosol Optical PROPERTIES over North China in Spring. *Int. J. Remote Sens.* 9: 429–437.

Zhao, T.X.P., Stowe, L.L., Smirnov, A., Crosby, S., Sapper, J. and McClain, C. (2002). Development of a Global Validation Package for Satellite Oceanic Aerosol Optical Thickness Retrieval Based on AERONET Observations and Its Application to NOAA/NESDIS Operational Aerosol Retrievals. *J. Atmos. Sci.* 59: 294–312.

Zheng, Y., Liu, J., Wu, R., Li, Z., Wang, B. and Tamio, T. (2008). Seasonal Statistical Characteristics of Aerosol Optical Properties at a Site near a Dusty Region in China. *J. Geophys. Res.* 113: D16205, doi: 10.1029/2007JD009384.

Received for review, May 13, 2013
Accepted, July 27, 2013